

## **Selective Cleavage of Nuclear Autoantigens During CD95 (Fas/APO-1)-mediated T Cell Apoptosis**

By Carlos A. Casiano,\* Seamus J. Martin,† Douglas R. Green,‡ and Eng M. Tan\*

From the \*W. M. Keck Autoimmune Disease Center, Department of Molecular and Experimental Medicine, The Scripps Research Institute, La Jolla, California 92037; and †Division of Cellular Immunology, La Jolla Institute for Allergy and Immunology, San Diego, California 92121

### **Summary**

Intracellular proteases appear to be important mediators of apoptosis. Substrates cleaved by proteases during apoptosis include nuclear autoantigens targeted in systemic autoimmune diseases. Using human autoantibodies as probes, we demonstrate here that T cell apoptosis mediated by CD95 (Fas/APO-1) is associated with substantial cleavage of a subset of nuclear autoantigens (7 of 33 examined). This subset included poly (ADP-ribose) polymerase, the 70-kD protein of the U1 small nuclear ribonucleoprotein particle, lamin B, the nuclear mitotic apparatus protein NuMA, DNA topoisomerases I and II, and the RNA polymerase I upstream binding factor UBF. Several of the cleaved autoantigens are involved in ensuring the integrity and proper conformation of DNA in the nucleus through interactions with the nuclear matrix, suggesting the possibility that their cleavage may contribute to the collapse of nuclear structure during apoptosis. The relative cleavage kinetics indicated that the autoantigens were targeted at various times after induction of apoptosis, suggesting either differential accessibility or activation of distinct proteases during the cell death process. These data reinforce the hypothesis that apoptosis is accompanied by selective cleavage of key substrates and not by a generalized degradation of intracellular material.

The activation of proteases is an important event in the control of apoptosis (1). These proteases include members of the interleukin-1 $\beta$ -converting enzyme (ICE)/CED-3 family, serine proteases, calpains, and granzymes (1). Major challenges in the analysis of proteolytic events associated with apoptosis are to define the mechanisms leading to protease activation, to characterize the different protease activities acting at various stages of apoptosis, and to identify key substrates whose cleavage might be linked to the profound changes in cellular architecture associated with this cell death process. Among the substrates cleaved during apoptosis are nuclear autoantigens targeted in systemic autoimmune diseases such as poly (ADP-ribose) polymerase (PARP) (2, 3), the 70-kD component of the U1 small nuclear ribonucleoprotein particle (U1-70 kD) (4), the nuclear lamins (5, 6), the nuclear matrix and mitotic apparatus protein NuMA (7, 8), and DNA-dependent protein kinase (9). It has been suggested that cleavage of certain autoantigens during apoptosis may reveal immunocryptic epitopes that could potentially induce autoantibody responses in systemic autoimmune diseases (9). In this study we used human autoantibodies as probes for the identification of substrates cleaved during CD95 (Fas/APO-1)-mediated T cell apoptosis. CD95-mediated cell death is involved in the regulation of immune reactions as

well as in T cell-mediated cytotoxicity (10). The importance of this cell death pathway in immune regulation is underscored by the demonstration that defects in the genes encoding CD95 and its ligand, CD95 L, are associated with autoimmune lymphoproliferative disorders in certain murine strains and in humans (10). Here we show that CD95-mediated apoptosis is accompanied by selective targeting of nuclear autoantigens by proteases acting at different stages of the cell death process.

### **Materials and Methods**

*Cell Lines and Reagents.* Jurkat and A1.1 cells (American Type Culture Collection, Rockville, MD) were cultured in RPMI 1640/10% fetal bovine serum under standard conditions. Anti-CD95/Fas mAb CH-11 was purchased from Medical and Biological Laboratories (Watertown, MA). Anti-CD3 mAb (145-2C11) was purified as described (11). Human sera containing highly specific, high titer autoantibodies to well characterized intracellular proteins were from the collection of the W.M. Keck Autoimmune Disease Center Laboratory serum bank. These sera were previously characterized by immunodiffusion, immunofluorescence microscopy, and immunoblotting in several studies performed in our laboratory. Rabbit antibody R29 reactive against the  $\alpha$  and  $\beta$  isoforms of DNA topoisomerase II was kindly provided by Dr. F.H. Drake (SmithKline Beecham, King of Prussia,

PA). Monoclonal antibody P4D2 to histone H2B was kindly provided by Dr. Robert L. Rubin (Scripps Research Institute, La Jolla, CA).

**Induction of Apoptosis.** Apoptosis was induced in Jurkat T cells by incubation with anti-CD95 mAb CH-11 at a final concentration of 100 ng/ml for up to 7 h. To minimize spontaneous apoptosis before incubation with anti-CD95 mAb, cell cultures were maintained in exponential growth by dilution in fresh medium every 2–3 d. Jurkat cells were also induced to undergo apoptosis by exposure to cycloheximide (75  $\mu$ M), C2-ceramide (40  $\mu$ M), actinomycin D (10  $\mu$ M), etoposide (150  $\mu$ M), and staurosporine (2  $\mu$ M) for 12 h. C2-ceramide was purchased from Biomol (Plymouth Meeting, PA). Staurosporine, etoposide (VP-16), actinomycin D, and cycloheximide were purchased from Sigma Chemical Co. (St. Louis, MO). A1.1 cells, a murine T cell hybridoma, were induced to undergo apoptosis by culturing in wells coated with an anti-CD3 mAb as previously described (11). Morphological changes associated with apoptosis, such as cell shrinkage, nuclear condensation and fragmentation, and plasma membrane blebbing were routinely monitored by light microscopy. Apoptotic cells were quantitated by fluorescence microscopic visualization of nuclei stained with 4',6-diamidino-2-phenylindole (DAPI).

**Electrophoresis and Western Blotting of Cell Lysates.** Cells were pelleted at 1,000 g for 10 min, followed by two washes in PBS containing the COMPLETE Protease Inhibitor Cocktail (Boehringer Mannheim, Germany). Cells were then resuspended at  $\sim 10^7$  cells/ml in lysis buffer containing 62.5 mM Tris-HCl, pH 6.8, 1% SDS, 10% glycerol, 1% mercaptoethanol, and the protease inhibitor cocktail. Lysates were boiled for 5 min to solubilize protein, passed through a 27-gauge needle to shear the DNA, and stored at  $-70^\circ\text{C}$  until required. Cell harvesting and lysate preparation were conducted in the presence of the protease inhibitor cocktail as a precaution to prevent further proteolysis. Total protein from  $\sim 10^6$  cells were separated by sodium dodecyl sulfate-polyacrylamide gel electrophoresis and transferred to nitrocellulose at 250 mA for 4–5 h. Immunoblotting was performed using standard procedures and detection of bound antibody was achieved by the enhanced chemiluminescence method (Amersham, Life Science, IL). Human sera were used at dilutions ranging from 1:100 to 1:500, depending on the antibody titer of the individual serum.

## Results

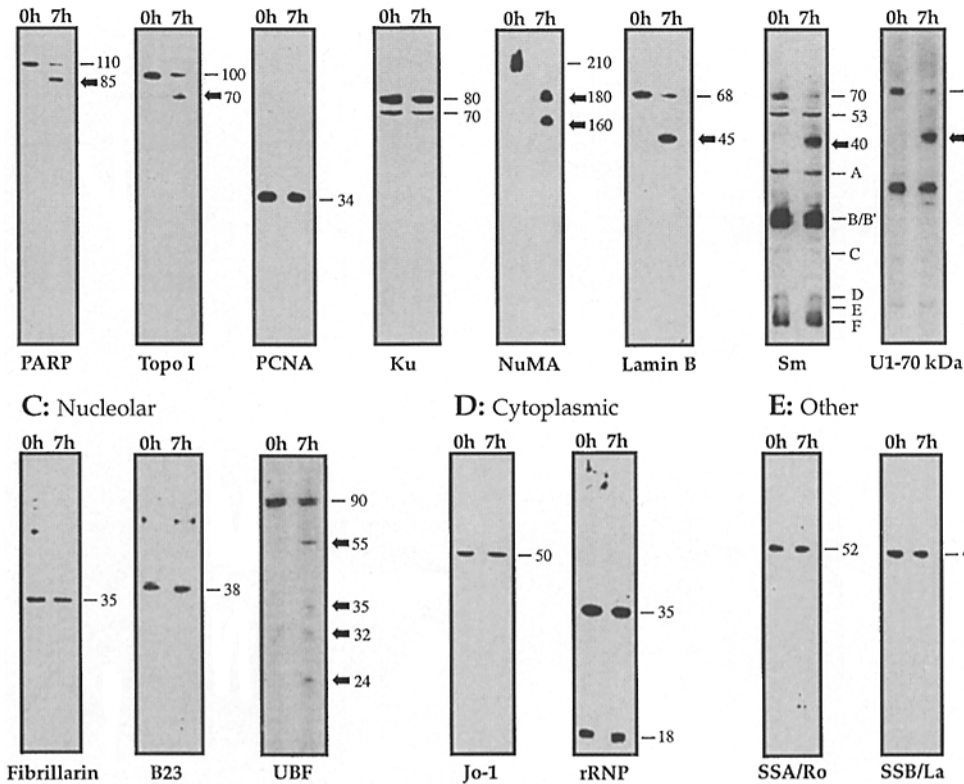
**Cleavage of a Subset of Nuclear Autoantigens during CD95-mediated Apoptosis.** 33 different autoantigens associated with

various subcellular structures and functions were examined by immunoblotting analysis of lysates from control and apoptotic Jurkat cells. Cells were induced to undergo apoptosis by incubation with anti-CD95 mAb (100 ng/ml). Approximately 60% of treated cells displayed the characteristic apoptotic morphology after 7 h of incubation with anti-CD95 mAb, as assessed by fluorescence microscopic examination of DAPI-stained nuclei (data not shown). DNA fragmentation was visible 2 h after addition of anti-CD95 antibody to cell cultures (data not shown).

Of 12 chromatin or DNA-associated proteins that were examined, PARP, DNA topo I, DNA topo II, NuMA, and lamin B (Table 1 and Fig. 1 A) underwent substantial cleavage during apoptosis, as judged by the appearance of lower molecular mass bands in the blots concomitant with a proportional reduction in the amount of the intact protein. PARP cleavage generated the signature 85-kD fragment reported previously (2, 3). DNA topo I cleavage yielded a 70-kD fragment. DNA topoisomerase II (both the  $\alpha$  and  $\beta$  isoforms) underwent extensive proteolysis that yielded several lower molecular mass fragments (Table 1; also see Fig. 2). NuMA, a nuclear matrix protein of 236 kD implicated in the organization of chromatin into loops via binding to specialized DNA sequences termed MARs (matrix attachment regions) (12), underwent complete proteolysis that yielded two fragments of  $\sim 180$  and 160 kD, respectively (Fig. 1 A). Lamin B, a nuclear envelope and also MAR-associated autoantigen (12) was cleaved into the signature 45-kD fragment reported previously (5, 6) (Fig. 1 A). Non-cleaved DNA/chromatin-associated autoantigens included PCNA, Ku, centromere proteins CENP A, CENP B, CENP C, histone H2B, and heterochromatin binding protein HP-1 (Fig. 1 and data not shown). Of 3 autoantigens associated with pre-mRNA splicing that were examined only U1-70 kD underwent substantial cleavage, yielding the 40-kD signature fragment described previously (4) (Fig. 1 B). None of the components of the Sm splicing particle were cleaved (Fig. 1 B). HCC1, a putative SR family splicing factor, was not cleaved (data not shown). Of 5 nucleolar-associated autoantigens examined (fibrillarin, B23/numatrin, To, PM-Scl, and UBF/NOR-90), only UBF underwent substantial proteolysis, which yielded fragments of 24, 32, 35, and 55 kD (Fig. 1 C and data not

**Table 1.** Nuclear Autoantigens Cleaved during CD95-mediated Apoptosis

Autoantigen	Associated functions	Proteolytic fragments
DNA topoisomerase I	Modification of DNA topology	70 kD
DNA topoisomerase II	Modification of DNA topology; anchoring chromatin to nuclear matrix	Multiple (125–160 kD)
Lamin B	Nuclear envelope formation; anchoring chromatin to nuclear matrix	45 kD
NuMA	Mitotic spindle formation; anchoring chromatin to nuclear matrix	160, 180 kD
PARP	DNA repair; interaction with chromatin in the nuclear matrix	85 kD
UBF/NOR-90	RNA pol I transcription; post-mitotic nucleolar organization	Multiple (24–55 kD)
U1-70 kD	pre-mRNA splicing; associated with the nuclear matrix (?)	40 kD

**A: DNA or chromatin associated**

**Figure 1.** Cleavage of a subset of autoantigens during CD95-mediated apoptosis of Jurkat cells. Representative blots of control and apoptotic lysates probed with various human autoimmune sera are shown. Intact proteins are indicated by lines, whereas proteolytic fragments are indicated by arrows. Numbers to the right of each blot represent relative molecular mass in kD. The anti-Sm serum also contained antibodies to U1-70 kD. The anti-U1-70 kD serum contained antibodies to a non-cleaved protein of 36 kD.

shown). Other non-cleaved autoantigens included SSA/Ro, SSB/La, p80 coilin, ribosomal proteins P0, P1, and P2, mitochondrial autoantigens PDCE2, X, OGDC, BCOADC, and E1 $\alpha$ , and tRNA synthetases Jo-1 (histidyl) and PL12 (alanyl) (Fig. 1 and data not shown).

**Relative Kinetics of Nuclear Autoantigen Cleavage after Induction of CD95-mediated Apoptosis.** To gain some insight into the relative sequence of proteolytic events during apoptosis we examined the kinetics of autoantigen cleavage after addition of anti-CD95 antibody to Jurkat cells. Substantial cleavage of PARP and NuMA was already detectable by 1 h (Fig. 2 A). These cleavages occurred before the appearance of appreciable numbers of apoptotic cells in the cultures. NuMA cleavage first yielded two fragments of  $\sim$ 190 and 180 kD, respectively. The 190-kD fragment disappeared after 3 h and a new fragment of  $\sim$ 160 kD began to accumulate. A short time-course experiment showed that PARP cleavage was already evident within 15 min of induction of apoptosis, whereas the cleavage of NuMA began shortly afterwards (data not shown). Lamin B was also targeted relatively early during apoptosis, as judged by the appearance of a small amount of the 46-kD fragment at 1 h. This cleavage progressed steadily and reached near completion by 7 h (Fig. 2 C). U1-70 kD cleavage occurred very rapidly between 1–2 h after induction of apoptosis since very low amounts of intact 70 kD were detected after 2 h (Fig. 2 D). Cleavage of DNA topo I was first visible by 2 h and was characterized by the appearance of 70- and 60-kD pro-

teolytic fragments. The 60-kD fragment was no longer detected after 3 h, whereas the amount of the 70 kD continued increasing as apoptosis progressed (Fig. 2 E). Substantial cleavage of the protein was not obvious until appreciable number of apoptotic cells (50–60%) had accumulated by 5–7 h. Cleavage of DNA topo II (both the  $\alpha$  and  $\beta$  forms) was evident at 3 h, as indicated by the decrease in the amount of the intact proteins, and by 7 h the protein was completely degraded into several smaller fragments (Fig. 2 F). Cleavage of UBF was first detected at 2 h by the appearance of a weak 58-kD band (Fig. 2 G) and progressed to generate fragments of 24, 32, and 35 kD. None of the Sm components were cleaved (Fig. 2 H).

**Cleavage of DNA Topo I Is Specifically Associated with Apoptosis.** The results presented above indicate that DNA topo I is a major substrate targeted by proteases during CD95-mediated apoptosis. Since it has been unclear in previous studies whether DNA topo I cleavage is specifically associated with apoptosis (9, 13, 14), we performed additional experiments aimed at demonstrating this association. We first examined whether DNA topo I cleavage could be inhibited under conditions where CD95-mediated apoptosis was inhibited. Jurkat cells were preincubated for 1 h in the presence of 10  $\mu$ M of a peptide inhibitor (Z-Val-Ala-Asp-fluoromethylketone; Z-VAD-fmk) of ICE/CED-3 proteases. Cells were then induced to undergo apoptosis by incubation with anti-CD95 mAb. Apoptosis was significantly inhibited in cells preincubated with Z-VAD-fmk (data not shown).

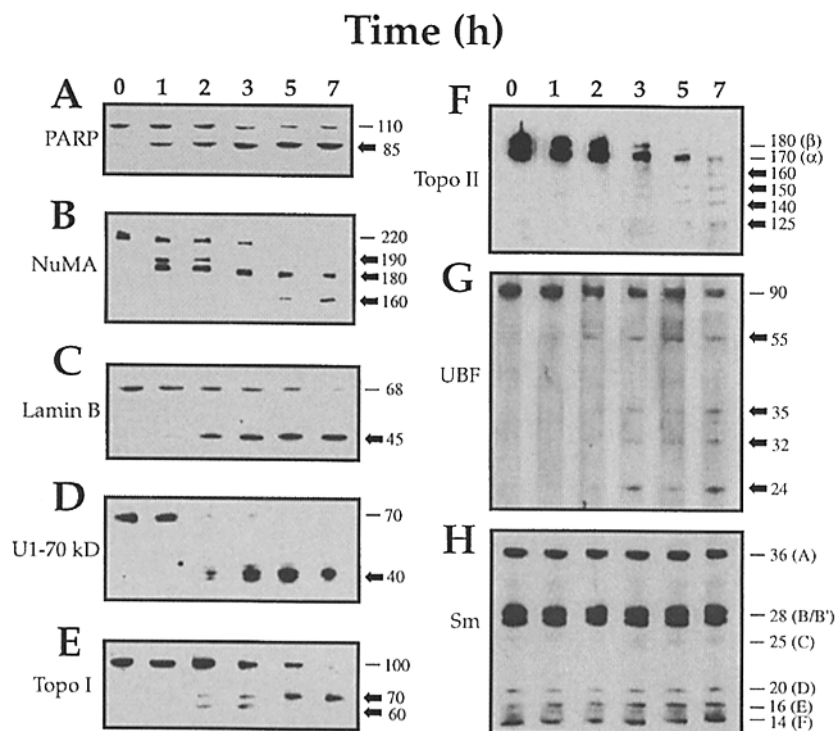


**Figure 2.** Kinetics of autoantigen cleavage after addition of anti-CD95 mAb to Jurkat cells. Intact proteins are indicated by lines, whereas proteolytic fragments are indicated by arrows. Numbers to the right of each blot represent relative molecular mass in kD. Results are representative of two independent experiments conducted under similar conditions.

Lysates from cells treated with anti-CD95 mAb alone revealed substantial cleavage of PARP and DNA topo I, whereas lysates from cells treated with the antibody in the presence of Z-VAD-fmk exhibited partial inhibition of PARP cleavage and complete inhibition of DNA topo I cleavage (Fig. 3). We also determined whether diverse apoptosis-inducing stimuli promoted cleavage of DNA topo I. Substantial cleavage of DNA topo I into the 70-kD fragment was detected after a 12 h exposure of Jurkat cells to apoptosis-inducing concentrations of C2-ceramide, etoposide (VP-16), actinomycin D, cycloheximide, and staurosporine (Fig. 4 A). Extensive cleavage of DNA topo I was also observed 6.5 h after induction of apoptosis in A1.1 cells with anti-CD3 mAb (Fig. 4 B). Typically, morphological characteristics of apoptosis appear in these cells within 3–4 h of incubation with the antibody, and 50–80% of the cells are apoptotic within 7–10 h (11). In contrast with the results obtained in Jurkat cells (see Figs. 1, 2 E, 3, and 4 A) this cleavage resulted in the generation of several proteolytic products ranging from 24 to 48 kD in addition to the 70-kD fragment, suggesting the possibility that various proteases might be involved in the cleavage of this protein in A1.1 cells.

## Discussion

These findings underscore the use of human autoantibodies as valuable tools for defining the various proteolytic events associated with apoptosis and strengthen the notion that this cell death process is accompanied by selective proteolysis of key substrates and not by generalized intracellu-

lar degradation. Although the exact role of the proteolytic cleavages described here in the execution phase of apoptosis remains to be established, it is noteworthy that most of the cleaved autoantigens are involved in ensuring the integrity and proper conformation of DNA in the nucleus or are associated with the nuclear matrix (Fig. 1; Table 1). This suggests the possibility that some of these cleavages could contribute to the collapse of nuclear matrix structure

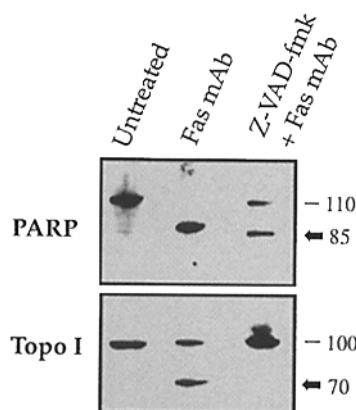


**Figure 3.** Inhibition of proteolytic cleavage of PARP and DNA topo I under conditions where apoptosis is inhibited. Jurkat cells were pre-incubated in the presence or absence Z-VAD-fmk (10  $\mu$ M) for 30 min before addition of anti-CD95 antibody. Nitrocellulose blots of cell lysates from control cells, cells treated with anti-CD95 mAb alone for 7 h, and cells pre-incubated with Z-VAD-fmk and then treated with anti-CD95 mAb for 7 h, were reactive with human autoantibodies to PARP and DNA topo I.

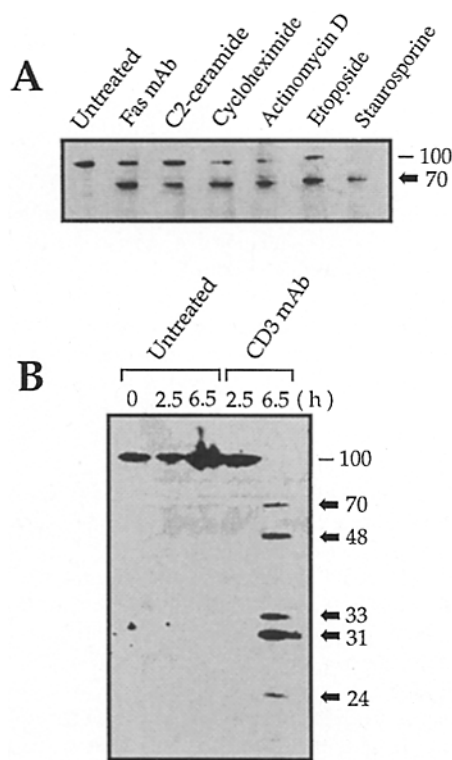


**Figure 4.** Cleavage of DNA topoisomerase I during apoptosis induced by different stimuli. (A) Cleavage of DNA topoisomerase I in Jurkat cells induced to undergo apoptosis by incubation with anti-CD95 mAb for 7 h, or by incubation with C2-ceramide (40  $\mu$ M), cycloheximide (75  $\mu$ M), actinomycin D (10  $\mu$ M), etoposide (150  $\mu$ M), and staurosporine (2  $\mu$ M) for 12 h. (B) Cleavage of DNA topoisomerase I during anti-CD3-induced apoptosis of A1.1 cells.

thereby facilitating chromatin degradation and nuclear fragmentation.

This study demonstrates conclusively that UBF, DNA topoisomerase I, and DNA topoisomerase II are major targets of proteases during CD95-mediated apoptosis. The apoptotic degradation of DNA topoisomerase I and DNA topoisomerase II had been reported in an earlier study but the cleavage products were not identified and the cleavage kinetics were not established (13). Two subsequent studies suggested that DNA topoisomerase I cleavage during apoptosis is minimal or non-specific (9, 14). We observed, however, that DNA topoisomerase I cleavage was specific, substantial, and tightly coupled to apoptosis since it could be inhibited under conditions where CD95-mediated apoptosis was blocked, was detected during apoptosis induced

by a variety of stimuli, and was not observed in control lysates. These discrepancies could be attributed to differences in the kinetics of the apoptosis systems and in the experimental conditions employed to induce apoptosis.

The observed differences in the relative kinetics of autoantigen cleavage suggests either differential accessibility or activation of distinct proteases during the cell death process. The identity of the protease(s) responsible for most of these cleavages remains unclear, although ICE/CED-3 proteases have been shown to cleave PARP and U1-70 kD in vitro (2-4). The cleavage of NuMA and DNA topoisomerase I into discrete fragments implies that they were targeted by proteases cleaving at specific sites, whereas the cleavage of DNA topoisomerase II and UBF into multiple fragments suggests that various proteases might be targeting these proteins. Although it is possible that DNA topoisomerases and UBF were cleaved by lysosomal proteases during advanced stages of CD95-mediated apoptosis, the fact that several other intracellular proteins remained intact during these stages clearly indicated a high degree of specificity in the proteolytic targeting of these autoantigens. It would be of interest to determine whether ICE/CED-3 proteases also participate in the late cleavage events involving the DNA topoisomerases and UBF.

It has been suggested that apoptosis-associated cleavage may enhance the immunogenicity of autoantigens by revealing immunocryptic epitopes that are not efficiently generated during antigen processing (9). The fact that many proteins that are frequently targeted by autoantibodies in human systemic autoimmune diseases are not cleaved during apoptosis (9 and this study) suggests that this putative mechanism, if operational, may be limited only to specific autoantigens. The presence of non-cleaved autoantigens in apoptotic bodies or blebs, such as SSA/Ro and SSB/La (15), suggests that alternative mechanisms might be operating to render released intracellular antigens immunogenic. It is possible that autoantibody responses could be amplified and maintained upon repeated stimulation by antigens due to unregulated or aberrant apoptosis, prolonged necrosis, defective phagocytic processing and presentation of debris from dying cells, or even antigen overexpression. It would be important not only to assess the immunogenic potential of subcellular particles and of proteolytic fragments released during cell death but also to investigate possible defects leading to aberrant apoptosis or phagocyte function, or antigen overexpression in systemic autoimmune diseases.

We thank Dr. K. Michael Pollard for helpful discussions and suggestions, Dr. Ri-Yao Yang for providing Jurkat cells, and Carol Peebles for assisting in the selection of some of the human sera.

C.A. Casiano was supported by a postdoctoral research fellowship from the Arthritis Foundation. S.J. Martin is a Wellcome Trust Fellow (041080). This work was supported in part by grants from the National Institutes of Health. This is publication number 10003-MEM from The Scripps Research Institute.

## References

1. Patel, T., G.J. Gores, and S.H. Kaufmann. 1996. The role of proteases during apoptosis. *FASEB J.* 10:587–597.
2. Tewari, M., L.T. Quan, K. O'Rourke, S. Desnoyers, Z. Zeng, D.R. Beidler, G.G. Poirier, G.S. Salvesen, and V.M. Dixit. 1995. Yama/CPP32 $\beta$ , a mammalian homolog of CED-3, is a CrmA-inhibitable protease that cleaves the death substrate poly(ADP-ribose) polymerase. *Cell.* 81:801–809.
3. Nicholson, D.W., A. Ali, N.A. Thornberry, J.P. Vaillancourt, C.K. Ding, M. Gallant, Y. Gareau, P.R. Griffin, M. Labelle, Y.A. Lazebnik et al. 1995. Identification and inhibition of the ICE/CED-3 protease necessary for mammalian apoptosis. *Nature (Lond.)*. 376:37–43.
4. Casciola-Rosen, L., D.W. Nicholson, T. Chong, K.R. Rowan, N.A. Thornberry, D.K. Miller, and A. Rosen, 1996. Apopain/CPP32 cleaves proteins that are essential for cellular repair: a fundamental principle of apoptotic cell death. *J. Exp. Med.* 183:1957–1964.
5. Oberhammer, F.A., K. Hochegger, G. Froschl, R. Tiefenbacher, and M. Pavelka. 1994. Chromatin condensation during apoptosis is accompanied by degradation of lamin A+B, without enhanced activation of cdc2 kinase. *J. Cell Biol.* 126: 827–837.
6. Neamati, N., A. Fernandez, S. Wright, J. Kiefer, and D.J. McConkey. 1995. Degradation of lamin B1 precedes oligonucleosomal DNA fragmentation in apoptotic thymocytes and isolated thymocyte nuclei. *J. Immunol.* 154:3788–3795.
7. Weaver, V.M., E.C. Carson, P.R. Walker, N. Chaly, B. Lach, Y. Raymond, D.L. Brown, and M. Sikorska. 1996. Degradation of nuclear matrix and DNA cleavage in apoptotic thymocytes. *J. Cell Sci.* 109:45–56.
8. Hsu, H.-L., and N.-H. Yeh. 1996. Dynamic changes of NuMA during the cell cycle and possible appearance of a truncated form of NuMA during apoptosis. *J. Cell Sci.* 109: 277–288.
9. Casciola-Rosen, L.A., G.J. Anhalt, and A. Rosen. 1995. DNA-dependent protein kinase is one of a subset of autoantigens specifically cleaved early during apoptosis. *J. Exp. Med.* 182:1625–1634.
10. Nagata, S., and P. Golstein. 1995. The Fas death factor. *Science (Wash. DC)*. 267:1449–1456.
11. Shi, Y., B.M. Sahai, and D.R. Green. 1989. Cyclosporin A inhibits activation-induced cell death in T cell hybridomas and thymocytes. *Nature (Lond.)*. 339:625–626.
12. Luderus, M.E.E., J.L. den Blaauwen, O.J.B. de Smit, D.A. Compton, and R. van Driel. 1994. Binding of matrix attachment regions to lamin polymers involves single-stranded regions and the minor groove. *Mol. Cell. Biol.* 14:6297–6305.
13. Kaufmann, S. H. 1989. Induction of endonucleolytic DNA cleavage in human acute myelogenous leukemia cells by etoposide, camptothecin, and other cytotoxic anticancer drugs: a cautionary note. *Cancer Res.* 49:5870–5878.
14. Voelkel-Johnson, C., A.J. Entingh, W.S.M. Wold, L.R. Gooding, and S.M. Laster. 1995. Activation of intracellular proteases is an early event in TNF-induced apoptosis. *J. Immunol.* 154:1707–1716.
15. Casciola-Rosen, L.A., G. Anhalt, and A. Rosen. 1994. Autoantigens targeted in systemic lupus erythematosus are clustered in two populations of surface structures on apoptotic keratinocytes. *J. Exp. Med.* 179:1317–1330.